Designing a heterostructure for the quantum receiver

A. A. Kiselev[a] and K. W. Kim
Department of Electrical and Computer Engineering, North Carolina State University, Raleigh, North Carolina 27695-7911

E. Yablonovitch
Department of Electrical Engineering, University of California, Los Angeles, Los Angeles, California 90024

(Received 27 December 2001; accepted for publication 4 March 2002)

In this letter, we develop optimal parameters for a structure which is suitable for the realization of a coherent quantum receiver. Conditions including predefined photon wavelength, strain, small Zeeman splitting of the electron levels, and large Zeeman effect for quantum-confined light holes are satisfied simultaneously for the structure based on the InGaAsP solid solutions. We are able to achieve designs with wavelengths of 1.3 and 1.55 μm that are desirable for optoelectronic applications. © *2002 American Institute of Physics.* [DOI: 10.1063/1.1472480]

The idea of secure quantum communications relies on entanglement of coherent quantum states.[1] To achieve this for practical use, one must be able to transmit quantum information over long distances, perform quantum operations to execute error correction, and retain the information without decoherence. Accounting for these demands, we have proposed a device that is capable of receiving quantum information in the form of coherent photon states, storing the information in the form of electron spin and/or performing the necessary operations, and then retransmitting the photon signal while maintaining quantum coherence throughout the whole process.[2] The core functionality of this device relies on the possibility to transfer information delivered in the form of photon polarization to electron spin in semiconductors and vice versa via absorption/emission processes.[3]

The design of the proposed receiver needs to satisfy several demanding conditions simultaneously. The first requires that both electron sublevels should couple optically to a single hole state, thus excluding entanglement with the quickly relaxing hole spin. That can be achieved by splitting valence band states with an external magnetic field. The splitting should be sufficiently large in order to resolve hole sublevels spectroscopically. As the applied magnetic field will also act on the electron states, their Zeeman splitting, in turn, should be smaller than the incident photon broadening, Γ_{ph}. Thus, the following inequality should be satisfied:

$$\delta H_{B,c} \equiv \mu_B g_c B \ll \Gamma_{\mathrm{ph}} \ll \mu_B g_v B \equiv \delta H_{B,v} . \tag{1}$$

Here indices "c" and "v" stand for conduction and valence bands, respectively. The spin splitting factor (or g factor) defines the influence of the external magnetic field on the doublet of otherwise degenerate states with opposite spins. As both left and right parts of Eq. (1) scale linearly with the magnetic field B (that is typically correct in small to moderate fields), it is sufficient that the linear dependence of the Zeeman effect still holds at the desired fields and that $g_c \ll g_v$. To get the feeling of the numbers involved, we provide here one estimate: $\delta H_B \approx 0.057$ meV for states with g factor $g=1$ in the magnetic field $B=1$ T. The values 0.1–0.3 meV are not unusual for Γ_{ph}.

The other two constrains are also required for lossless transfer of information encoded in the form of photon polarization into the electron spin. The suitable selection rules, allowing this transfer in heterostructures based on the semiconductors with the zinc-blende symmetry, take place only in the case of (a) in-plane magnetic field and (b) for the electron–light hole (LH) transitions (see Ref. 2 for a more thorough explanation of these requirements). The condition (b) can be fulfilled in a strained heterostructure (in order to make the LH the ground state). However, possible strain-related technical problems need to be accounted for in the structure design in this case.

And last but not least, it is our obvious desire to use modern fiber optics data communication systems as a prototype, which sets additional requirement on the energy of the optical interband transitions.

Now we attempt to satisfy all the earlier mentioned conditions simultaneously. A comprehensive theory of the Zeeman effect in crystals and semiconductor heterostructures is already well established.[4–6] Detailed formulas for electron g factor in strained cubic heterostructures are given in Ref. 7. Equations for the LH g factor obtained in the framework of the 8×8 **kp** model were also recently published.[8] Energies of the confined states in the conduction and valence bands of the strained heterostructure are routinely obtained as a part of the g factor calculation procedures.

In addition to the calculation scheme in Refs. 6 and 7, we have also included into the electron Hamiltonian the free electron mass and the remote bands contribution to the dispersion of the conduction electrons. This provides much better accuracy in determining electron quantization energies and, as a consequence, optical transition energies.

Analyzing parameters of various semiconductor materials, we have concluded that the structures based on the family of $In_{1-x}Ga_xAs_yP_{1-y}$ solid solutions are the most promising candidates due to the uniquely broad variety of the band gaps encompassing important optical frequencies, moderate deviation in the lattice constants, and drastically different

[a]Electronic mail: kiselev@eos.ncsu.edu

 © 2002 American Institute of Physics

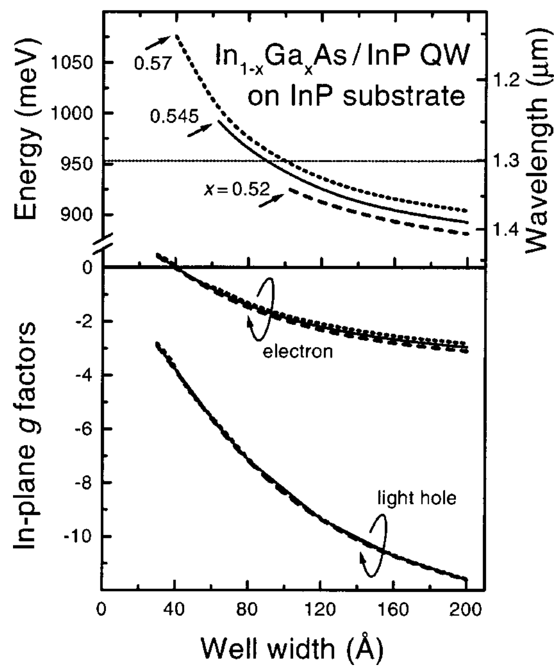

FIG. 1. Optical transition energies and g factors for $In_{1-x}Ga_xAs/InP$ QW structures grown on InP.

strengths of the intrinsic spin-orbit (SO) effect delivered by different compositions. Though not independent, variety in the band gap and SO interaction provides substantial flexibility desirable in the band structure and g factor engineering. Variation of the lattice constant opens doors to the strain engineering as an additional leverage for optimization.

Material parameters for the constituent binary compounds are obtained from Ref. 9. For solid solutions, we utilize the interpolation scheme of Ref. 8. However, for the deformation potential constants, we adopted the numbers for binary compounds from Vurgaftman *et al.*[10] instead of using the same typical values for all compounds.[8] This modification produces a minor but noticeable effect on the LH g factor values.

Now we describe the main results of the present letter that are summarized in Fig. 1. Data sets for the three different compositions of the $In_{1-x}Ga_xAs$ well layer ($x=0.52$—dashed, 0.545—solid, and 0.57—dotted lines) are shown as a function of the quantum well (QW) width. Energies of the electron-LH optical transitions are given in the upper part of the graph; due to the effects of spatial confinement the energy values increase with the decreasing layer thicknesses. For a larger Ga content, the band gap of the InGaAs solid solution also becomes larger, which explains the relative position of these three curves (strain effects that are very important for the alignment of valence states are typically smaller in magnitude). Special meaning is assigned to the leftmost point of each curve (also marked by an arrow). It gives a crossover point of the electron-LH and electron-heavy hole (HH) transitions: at the widths to the left of this point, quantum confinement is so strong that it alone defines the order of LH and HH states, and a HH with a larger mass forms the ground hole state. To the right, energy separation due to confinement is smaller than the strain-induced splitting in the valence band. Here, the LH forms the ground hole state and this is the region of our interest. For $x=0.47$, the lattice constant of InGaAs matches exactly to that of InP and the crossover point does not exist for this heteropair (or, more accurately, it is shifted to infinity). Beyond 0.47, the crossover point occurs at the smaller and smaller well widths, as the lattice constant mismatch increases (see Fig. 1). For example, the in-plane biaxial tensile strain ε_{xx} reaches 0.63% for $x=0.57$. It is probably impractical to implement structures with a large mismatch as that would quickly reduce critical layer thicknesses and limit flexibility in the structure design. As for the position of the crossover point, it already takes place in narrow wells of only ~40 Å even for $\varepsilon_{xx}=0.63\%$. Returning to the essence of the design requirements, one can note that the energy of the electron-LH optical transition in these structures can easily be adjusted to the 1.3 μm transparency window of the contemporary fibers.

The lower part of the graph shows the results of g factor calculations for both electron and LH states in the QW (for the case of in-plane magnetic field). Both electron and LH dependencies saturate in wide wells (asymptotically reaching bulk values, adjusted by strain) and grow from more negative to less negative and even to positive values as the QW shrinks. It turns out that in our structures the electron g factor component becomes zero at a well width larger than that of the LH and in the vicinity of this point we obtain a very high ratio of the electron to LH Zeeman splittings (i.e., $g_c \ll g_v$). As the well thickness increases further, the ratio becomes smaller, but nevertheless always exceeds 3–3.5 for the considered InGaAs/InP samples. That is indeed a very important result because with such a difference in the g factor values Eq. (1) is guaranteed to be satisfied (in a proper magnetic field).

We also note that, quite surprisingly, the LH g factor is practically insensitive to the QW layer composition when confinement and strain effects are both accounted for (with the adopted deformation potential values recently compiled by Vurgaftman *et al.*[10]) We attribute this phenomenon to the coincidental interplay of several competing factors; it definitely should not be considered as a universal rule.

Thus, InGaAs/InP heterostructures fulfill all the requirements of the quantum receiver design. As we can see in Fig. 1, optical band gap can be tuned to match photon wavelength $\lambda \sim 1.3$ μm. However, it is not true for the 1.55 μm wavelength that is indeed very desirable.

Now we come to the most challenging part of this effort. With no space above $y=1$ on the (x,y) plane representing arbitrary $In_{1-x}Ga_xAs_yP_{1-y}$ solid solutions, one can try to achieve further reduction of the structure optical bandgap with the well layer compositions to the left of the line $x=0.47y$, defining InGaAsP solid solutions lattice matched to InP. Grown on InP substrate, though, these layers would have unacceptable order of valence band hole states. Hence, it is important to use a substrate material with a lattice constant even larger than InP. We explore the structures with the following design: a substrate that defines the in-plane lattice constant of the whole structure, relatively thin InP barriers, and a InGaAs well layer between them. Figure 2 shows the results for three structures with the different substrate materials and, consequently, different in-plane strain $\varepsilon_{xx,\mathrm{InP}}$ in the InP layers: 0% (dotted—identical to Fig. 1), 0.5% (solid),

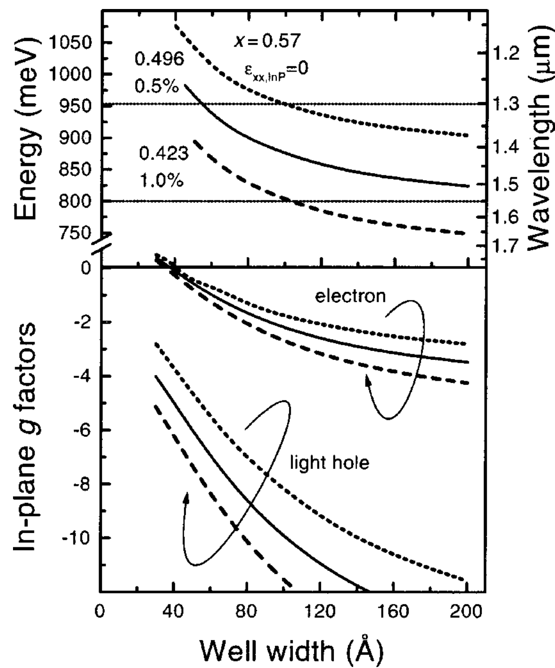

FIG. 2. Optical transition energies and g factors for $In_{1-x}Ga_xAs$/InP QW structures grown on a thick buffer layer with a larger (than InP) lattice constant.

and 1.0% (dashed lines). The QW layer composition x is correspondingly adjusted to keep strain in this layer at the fixed value of $\varepsilon_{xx}\approx 0.63\%$ in all three structures. As in Fig. 1, the curves in the upper part of the graph represent the electron-LH transition energy as a function of the well thickness. Due to the smaller Ga content in the material of the well layer, we are able to reach smaller optical transition energies, now overlapping the $\lambda \sim 1.55\ \mu$m range as well. The leftmost point of each of these lines again identifies the crossover point of the LH and HH subbands. As expected, the position of this point is pretty much the same in all three structures, since it is only slightly affected by the strain in the InP barrier layers and the well layer strain is fixed. Concerning the electron and LH g factor dependencies, we obtained qualitatively similar behavior to the one shown in Fig. 1, with somewhat better ratio overall (actually, consistently better than 4).

Up till now we have not discussed an actual choice of the material for the buffer layer. The most obvious candidates would be $InAs_xP_{1-x}$ and $In_{1-x}Al_xAs$ (though the later introduces yet another cation into the heterosystem). Arsenic content $x\approx 0.2$ in InAsP corresponds to the $\varepsilon_{xx,\mathrm{InP}}=0.5\%$ while $x\approx 0.4$ would give the in-plane strain in the InP layer on the order of 1%. Both of these compositions have band gaps larger than the targeted 0.954 and 0.8 eV, respectively, preventing leakage of the electron from the QW confined level. Unfortunately, the substrates made from these materials are not available and, as a result, one needs to start with the InP wafer. Both InAsP and InAlAs are confirmed to grow well on the conventional InP substrates. There will be a break in the pseudomorphic growth when layers reach critical thicknesses to establish their own lattice constant. If necessary, the developed threading dislocations can be terminated by incorporating short period superlattices/stop layers, composition grading, epilayer tilting (dislocation bending techniques), special temperature regime of growth with low-temperature portions, general optimization of the growth conditions, or other methods. On the other hand, we are interested in a device with a very small area. With the best achievable dislocation densities currently in the range of $10^6-10^7\ \mathrm{cm}^{-2}$, it should be possible to identify and utilize a region of the structure with no dislocations nearby. An innovative technique involving structure patterning with the subsequent annealing was recently shown to allow complete removal of the threading dislocations (supposedly due to the thermally activated glide of dislocations to the sidewalls of patterned regions).[11]

In summary, we have designed a practical QW structure that would satisfy all requirements of the proposed quantum receiver. Detailed structure parameter maps are established for structures based on InGaAsP family of semiconductor solid solutions.

A.A.K. would like to thank S. Bedair and S. V. Ivanov for helpful discussions. This work was supported, in part, by the Defense Advanced Research Projects Agency and the Office of Naval Research.

[1] A. Zeilinger, Phys. World 35 (1998); W. Tittel, G. Ribordy, and N. Gisin, *ibid.* 41 (1998).
[2] R. Vrijen and E. Yablonovitch, Physica E (Amsterdam) **10**, 569 (2001).
[3] G. E. Pikus and A. N. Títkov, in *Optical Orientation*, edited by F. Meier and B. P. Zakharchenya (Elsevier, New York, 1994), p. 73.
[4] L. M. Roth, B. Lax, and S. Zwerdling, Phys. Rev. **114**, 90 (1959).
[5] E. L. Ivchenko and A. A. Kiselev, Sov. Phys. Semicond. **26**, 827 (1992).
[6] A. A. Kiselev, E. L. Ivchenko, and U. Rössler, Phys. Rev. B **58**, 16353 (1998).
[7] A. A. Kiselev, K. W. Kim, and E. L. Ivchenko, Phys. Status Solidi B **215**, 235 (1999).
[8] A. A. Kiselev, K. W. Kim, and E. Yablonovitch, Phys. Rev. B **64**, 125303 (2001).
[9] *Intrinsic Properties of Group IV Elements and III–V, II–VI, and I–VII Compounds*, Landolt-Börnstein, New Series, Group III Vol. 22, Pt. A, edited by O. Madelung (Springer, Berlin, 1987); *Semiconductors—Basic Data*, edited by O. Madelung (Springer, Berlin, 1996).
[10] I. Vurgaftman, J. R. Meyer, and L. R. Ram-Mohan, J. Appl. Phys. **89**, 5815 (2001).
[11] X. G. Zhang, A. Rodriguez, P. Li, F. C. Jain, and J. E. Ayers, J. Electron. Mater. **30**, 667 (2001).